DOI: 10.1002/chem.200901238

Enhanced Reactivities of Iron(IV)-Oxo Porphyrin π-Cation Radicals in Oxygenation Reactions by Electron-Donating Axial Ligands

Yaeun Kang,[a] Hui Chen,[b] Yu Jin Jeong,[a] Wenzhen Lai,[b] Eun Hae Bae,[a] Sason Shaik,*[b] and Wonwoo Nam*[a]

Dedicated to Professor Joachim Sauer on the occasion of his 60th birthday

Abstract: The proximal axial ligand in heme iron enzymes plays an important role in tuning the reactivities of iron(IV)-oxo porphyrin π-cation radicals in oxidation reactions. The present study reports the effects of axial ligands in olefin epoxidation, aromatic hydroxylation, alcohol oxidation, and alkane hydroxylation, by $[(tmp)^{+\bullet}Fe^{IV}(O)(p\text{-Y-PyO})]^{+}$ (**1**-Y) (tmp = *meso*-tetramesitylporphyrin, *p*-Y-PyO = *para*-substituted pyridine *N*-oxides, and Y = OCH_3, CH_3, H, Cl). In all of the oxidation reactions, the reactivities of **1**-Y are found to follow the order **1**-OCH_3 > **1**-CH_3 > **1**-H > **1**-Cl; negative Hammett ρ values of −1.4 to −2.7 were obtained by plotting the reaction rates against the σ_p values of the substituents of *p*-Y-PyO. These results, as well as previous ones on the effect of anionic nucleophiles, show that iron(IV)-oxo porphyrin π-cation radicals bearing electron-donating axial ligands are more reactive in oxo-transfer and hydrogen-atom abstraction reactions. These results are counterintuitive since iron(IV)-oxo porphyrin π-cation radicals are electrophilic species. Theoretical calculations of anionic and neutral ligands reproduced the counterintuitive experimental findings and elucidated the root cause of the axial ligand effects. Thus, in the case of anionic ligands, as the ligand becomes a better electron donor, it strengthens the FeO−H bond and thereby enhances its H-abstraction activity. In addition, it weakens the Fe=O bond and encourages oxo-transfer reactivity. Both are Bell–Evans–Polanyi effects, however, in a series of neutral ligands like *p*-Y-PyO, there is a relatively weak trend that appears to originate in two-state reactivity (TSR). This combination of experiment and theory enabled us to elucidate the factors that control the reactivity patterns of iron(IV)-oxo porphyrin π-cation radicals in oxidation reactions and to resolve an enigmatic and fundamental problem.

Keywords: axial ligand effect · density functional calculations · enzyme models · porphyrinoids · two-state reactivity

Introduction

High-valent iron(IV)-oxo porphyrin species have been implicated as key intermediates in the catalytic cycles of heme iron enzymes, such as cytochromes P450, peroxidases, and catalases.[1] In these enzymes, proximal axial ligands are thought to play an important role in tuning the reactivities of iron(IV)-oxo porphyrin π-cation radicals, referred to as compound I (Cpd I).[2] In particularly, it has been proposed for thiolate-ligated enzymes that the electron donation from the axial ligand to the iron center increases the basicity of the iron-oxo group, thereby allowing a hydrogen atom to be abstracted from C–H bonds by Cpd I under mild conditions.[2b] This is an important hypothesis, which might explain the high reactivity of cytochrome P450 in C–H bond activation reactions. Thus, according to this hypothesis, one

[a] Y. Kang,[+] Y. J. Jeong,[+] E. H. Bae, Prof. Dr. W. Nam
Department of Chemistry and Nano Science
Department of Bioinspired Science, Centre for Biomimetic Systems
Ewha Womans University, Seoul 120-750 (Korea)
Fax: (+82) 2-32774441
E-mail: wwnam@ewha.ac.kr

[b] Dr. H. Chen,[+] Dr. W. Z. Lai,[+] Prof. Dr. S. Shaik
Institute of Chemistry and The Lise Meitner-Minerva Center for Computational Quantum Chemistry, The Hebrew University of Jerusalem, 91904 Jerusalem (Israel)
Fax: (+972) 2-6584680
E-mail: sason@yfaat.ch.huji.ac.il

[+] These authors contributed equally to this work.

Supporting information for this article is available on the WWW under http://dx.doi.org/10.1002/chem.200901238.

should expect that an increase in the electron donation property of the axial ligand will result in enhanced reactivity in C–H hydroxylation. This is, however, a counterintuitive reactivity trend for an essentially electrophilic species. In addition, it is not clear how this hypothesis would account for the axial ligand effect in oxo-transfer reactions (e.g., the oxidation of sulfides and phosphines), wherein the ferryl basicity effect is not really apparent. These questions are the focus of the present study that combines experimental and theoretical approaches to elucidate the effects of both anionic ligands, such as thiolate, and neutral ones, such as pyridine *N*-oxide, on the reactivities of model Cpd I complexes.[3–5]

A brief review of the current status of axial ligand effects in heme and nonheme systems is present in Figure 1, which schematizes the various available reactivity patterns. Thus, the reactivity of the nonheme iron(IV)-oxo complex, $[(tmc)Fe^{IV}(O)(X)]^{n+}$ (tmc = 1,4,8,11-tetramethyl-1,4,8,11-tetraazacyclotetradecane), is affected by the nature of anionic axial ligands (X^-) in opposite manners depending on the reaction types (Figure 1, left).[6] As can be seen, oxo-transfer reactivity correlates with the electrophilicity of the oxidant and is enhanced by electron-withdrawing ligands, whereas H-atom abstraction reactivity follows the opposite trend and is enhanced by electron-donating ligands. This dichotomy was theoretically interpreted based on the fact that nonheme iron(IV)-oxo reagents possess two closely lying spin states, a ground state with a triplet spin state (T), and a low-lying quintet spin state (Q). As such, the inverted reactivity in H-atom abstraction was ascribed to the increased contribution of the more reactive quintet state (e.g., blending of the triplet and quintet states or faster spin crossover for the better donor ligand).[7] By contrast, in the analogous ruthenium(IV)-oxo complexes, $[(tmc)Ru^{IV}(O)(X)]^{n+}$ (Figure 1, middle), in which the ground state is triplet and the quintet state is high lying showed that both reaction types were enhanced by electron-withdrawing ligands, in line with the increased electrophilicity of the Ru-oxo reagent.[8] Hence the electrophilic-reactivity trend in these complexes was shown to be an outcome of a single spin state reactivity, which is quite different from the iron reagent that proceeds through two-state reactivity (TSR).[3c] We note that the FeO–H bond

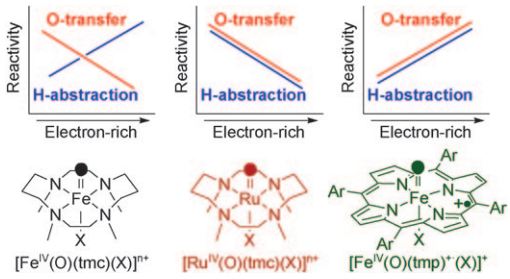

Figure 1. Schematic drawings showing the axial ligand effects on the reactivities of $[(tmc)Fe^{IV}(O)(X)]^{n+}$ (left), $[(tmc)Ru^{IV}(O)(X)]^{n+}$ (middle), and $[(tmp)^{+\bullet}Fe^{IV}(O)(X)]^{+}$ (X = *p*-Y-PyO) (right) in oxo-transfer (red line) and H-atom abstraction (blue line) reactions.

strengths in the $[(tmc)FeIV(O)(X)]^{n+}$ series were found to be constant,[7] and hence, the basicity of the ferryl could not possibly control these reactivity trends.

In heme systems, Cpd I species are known to carry out a variety of oxygenation processes.[3–5] So far, mostly anionic X ligands were investigated and found to exert a significant effect on the reactivity of Cpd I models (Figure 1, right).[4] For example, $[(Por)^{+\bullet}Fe^{IV}(O)(Cl)]$ (where Por is *meso*-tetrakis(pentafluorophenyl)porphyrin) is 650 times more reactive than $[(Por)^{+\bullet}Fe^{IV}(O)(CF_3SO_3)]$ in cyclohexane hydroxylation, which indicates that the activation of C–H bonds is markedly dependent on the anionic axial ligands of iron-oxo porphyrin oxidants.[4b] The axial ligand effects in heme iron models have, however, been less systematically investigated compared with the non-heme iron(IV)- and ruthenium(IV)-oxo complexes.[6–8] We therefore decided to complete this missing part of the puzzle by investigating the axial ligand effects with iron(IV)-oxo porphyrins bearing neutral *para*-substituted pyridine *N*-oxides in oxo-transfer and H-atom abstraction reactions and to discover the reactivity patterns that can establish the conditions for the dominance of the basicity hypothesis[2b] or of the TSR notion of reactivity[3c] in a given case. We hereby report that iron(IV)-oxo porphyrins bearing electron-donating axial ligands are more reactive in the oxo-transfer and H-atom abstraction reactions (Figure 1, right); the reactivity trends are different from those of nonheme iron(IV)- and ruthenium(IV)-oxo complexes.[6,8] The present results, as well as those previously obtained for anionic X ligands,[4b] are interpreted by using DFT calculations. This combination of experiment and theory enables us to shed light on the control of the reactivity patterns of iron(IV)-oxo porphyrin π-cation radicals in oxygenation reactions either by TSR or by basicity of the iron-oxo reagent.

Results and Discussion

Iron(IV)-oxo porphyrin π-cation radicals bearing *p*-substituted pyridine *N*-oxides (*p*-Y-PyO), $[(tmp)^{+\bullet}Fe^{IV}(O)(p\text{-Y-PyO})]^{+}$ (**1**-Y) (tmp = *meso*-tetramesitylporphyrin; Y = OCH_3, CH_3, H, Cl) were prepared by literature methods:[4a,c] $[Fe^{III}(tmp)](CF_3SO_3)$ was treated with 5 equivalents of *p*-Y-PyO, followed by the bubbling of ozone gas slowly through a solvent mixture of CH_3CN and CH_2Cl_2 (9:1) at −40 °C (see Figure 2a for UV/Vis spectra). Compound **1**-Y was then employed to perform various oxidation reactions, such as olefin epoxidation, aromatic hydroxylation, alcohol oxidation, and alkane hydroxylation. First, olefin epoxidation by **1**-Y was examined. Upon the addition of cyclohexene to **1**-Y, the intermediate reverted back to the starting iron(III) porphyrin complex with clear isosbestic points at 475 and 548 nm and showed pseudo-first-order decay as monitored by a UV/Vis absorption spectroscopy (Figure 2b). Pseudo-first-order fitting of the kinetic data allowed us to determine k_{obs} values and the pseudo-first-order rate constants were seen to increased proportionally with the substrate concentration and allowed us to determine second-order rate con-

stants (see Table S1, Supporting Information). Product analysis of the reaction mixture revealed that cyclohexene oxide was produced in high yields (~50% based on **1**-Y generated) and the product distribution was not affected by the axial ligands and reaction temperatures.[4b,9] Interestingly, by plotting the rates as a function of the σ_p values of the substituents of *p*-Y-PyO, a good linear correlation was obtained with a negative Hammett ρ value of −2.6(2) (Figure 2c). The latter result indicates that iron(IV)-oxo porphyrin π-cation radicals with electron-donating axial ligands are more reactive towards olefin epoxidation.

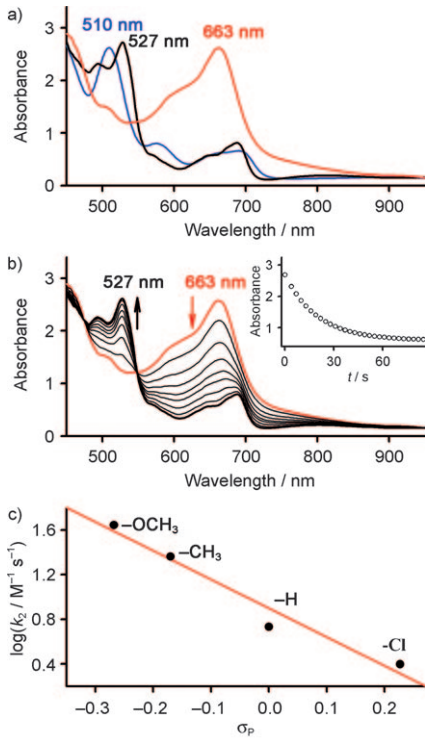

Figure 2. a) UV/Vis spectra of $[Fe^{III}(tmp)](CF_3SO_3)$ (0.20 mM) (blue line), $[Fe^{III}(tmp)](CF_3SO_3)$ + 5 equivalents of *p*-CH_3-PyO (black line), and $[(tmp)^{+\bullet}Fe^{IV}(O)(p\text{-}CH_3\text{-}PyO)]^+$ (**1**-CH_3) (red line). b) UV/Vis spectral changes of **1**-CH_3 (0.2 mM) upon the addition of 10 equivalents of cyclohexene at −40 °C. The inset shows the time course of the decay of **1**-CH_3 monitored at 663 nm. c) Plot of log k_2 of **1**-Y against σ_p of the substituents of *p*-Y-PyO in the epoxidation of cyclohexene.

The axial ligand effect was also investigated in aromatic hydroxylation, where an initial electrophilic attack on the π-system of the aromatic ring by iron(IV)-oxo porphyrin π-cation radicals was proposed by experimental and theoretical studies.[10] The reaction of **1**-Y with naphthalene afforded pseudo-first-order decay and the second-order rate constants were determined by varying the naphthalene concentration (Table S1). By plotting the second-order rate constants as a function of σ_p of the substituents of *p*-Y-PyO, a negative Hammett ρ value of −2.7(2) was obtained (Figure S1a). Similarly, a negative Hammett ρ value of −2.0(3) was obtained in the oxidation of benzyl alcohol by **1**-Y (Figure S1b; see also Table S1 for second-order rate constants), where the oxidation of alcohols by iron(IV)-oxo porphyrin π-cation radicals was proposed to occur by an α-CH hydrogen-atom abstraction, followed by electron transfer.[11] We therefore concluded that reactivities of iron(IV)-oxo porphyrin π-cation radicals are enhanced by electron-donating axial ligands in aromatic hydroxylation and alcohol oxidation reactions as well as in olefin epoxidation.

We then investigated the reactivities of **1**-Y in alkane hydroxylation reactions with substrates such as xanthene, 9,10-dihydroanthracene (DHA), fluorene, and ethylbenzene (PhEt). In all of the reactions, we observed pseudo-first-order decay of **1**-Y and were able to determine second-order rate constants (Table S1). The product analysis revealed the formation of good amounts of products, as reported in H-atom abstraction reactions by iron(IV)-oxo porphyrins.[12] Firstly, we observed that the rate constants decreased with an increase in the C–H bond dissociation energy (BDE) of the substrates (xanthene, 75.5 kcal mol^{-1}; DHA, 77 kcal mol^{-1}; fluorene, 80 kcal mol^{-1}),[13] and a good linear correlation with a slope of −0.43 was observed when the log k_2' values were plotted against the C–H BDE values of the substrates (the k_2 values are divided by the number of equivalent target C–H bonds of the substrates to obtain the k_2' values; Figure S2). This result indicated that the H-atom abstraction is the rate-determining step for the C–H bond activation of alkylaromatics.[14] Secondly, when the rates were plotted against the σ_p values of the substituents of *p*-Y-PyO, a negative Hammett ρ value of −1.4(2) was obtained in the reaction of xanthene (Figure S1c). This result demonstrates that the more electron-donating the axial ligand is, the more reactive the iron-oxo porphyrin species becomes in C–H bond activation reactions. Furthermore, the kinetic isotope effect (KIE) value of 6.5(3) was determined in the oxidation of xanthene by **1**-CH_3 (Figure S3) and this value is lower than that determined in the reactions of iron(IV)-oxo complexes of heme and non-heme ligands (e.g., KIE values of ~20).[6,12] We also observed the dependence of the KIE values on the axial ligands (e.g., *p*-Y-PyO; Y = OCH_3, CH_3, H, Cl), and obtained KIE values in the range of 4.7–10 (Table S2). In fact, the plot of KIE values against the σ_p value of the substituents of *p*-Y-PyO afforded a good linear correlation with a positive slope of 0.62 (Figure 3). Thus, the KIE values indicate that the more electron donating the Y group in **1**, the less advanced the transition state in terms of C–H cleavage, following similar observations from calculations on C–H hydroxylation by P450.[15] Finally, the axial ligand effect of **1**-Y was investigated in the hydroxylation of PhEt (Table S1 for second-order rate constants),[16] and a negative Hammett ρ value of −1.8(2) was obtained by plotting rates against σ_p values of the substituents of *p*-Y-PyO (Figure S1d). Thus, as observed in olefin epoxidation, aromatic hydroxylation, and alcohol oxidation, iron(IV)-oxo porphyrin π-cation radicals bearing more electron-donating axial ligands show greater reactivities in C–H bond activation reactions. In all of the above processes, however, the range of reactivity from the most electron-donating substituent to the most electron-withdrawing one is only 10-fold or

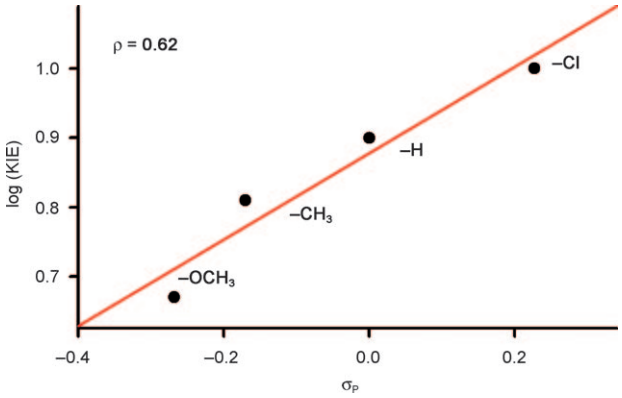

Figure 3. Plot of logKIE of **1**-Y against σ_p of the substituents of *p*-Y-PyO in the oxidation of xanthene by $[(tmp)^{+\bullet}Fe^{IV}(O)(p\text{-Y-PyO})]^{+}$.

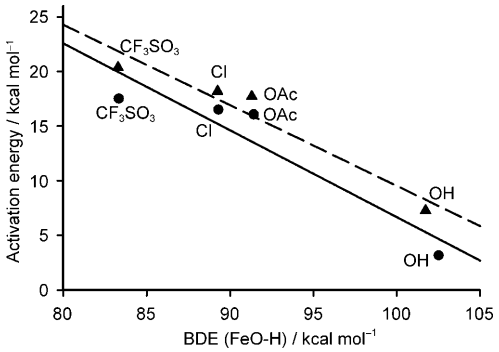

Figure 4. Activation energies for H-abstraction from cyclohexane versus BDE(FeO–H) of the O–H bond formed during the process. ● = doublet, ▲ = quartet.

so. This trend can be contrasted with the effect of anionic ligands in the same reaction types, which was found to be over 650-fold.[4b] As such, this study raises the following fundamental questions: a) Why is the reactivity effect in anionic ligands so much larger than in the neutral *p*-Y-pyridine *N*-oxide ligands? b) What are the origins of the observation that oxygenation reactivity of iron(IV)-oxo porphyrin π-cation radicals increases as the *p*-substituent of the pyridine *N*-oxide ligand becomes more electron donating? c) How are these trends associated with TSR and/or with the basicity hypothesis? These questions were tackled with the help of DFT calculations.

Theoretical studies: The DFT calculations were carried out for the following two systems; a) the reaction of $[(Por)^{+\bullet}Fe^{IV}(O)(X)]$ with cyclohexane in an H-abstraction reaction, where $X^- = CF_3SO_3^-$, Cl^-, AcO^-, HO^-, and b) the reaction of $[(tmp)^{+\bullet}Fe^{IV}(O)(p\text{-Y-PyO})]^{+}$ (Y = Me, Cl) with PhEt. The calculations employed the B3LYP functional using a previously published procedure,[7] as described in the Computational Methods Section. The key results at the B3LYP/B2 level are described here and the full details and results are given in the Supporting Information.

The first set of calculations showed that the anionic ligand had a very significant effect on hydrogen abstraction from cyclohexane, as observed in experiment.[4b] Thus, the total difference in activation barriers from $X^- = CF_3SO_3^-$ through to $X^- = HO^-$ was 13 kcal mol^{-1} or more. This was observed for the two spin states of Cpd I; the doublet and quartet spin states. Therefore, the computed reactivity patterns clearly follow the electron-donating power of the axial ligands as experimentally observed.[4b]

To understand the underlying factors of this pattern, a plot of the computed activation barriers for H-abstraction from cyclohexane against the BDE(FeO–H) of the O–H bond, formed during H-abstraction by Cpd I, is shown in Figure 4. It is seen that the correlation is linear, as predicted by the Bell–Evans–Polanyi (BEP) principle[17] and found extensively in experimental systems by Mayer.[13,14a] Clearly, as the axial ligand becomes a better electron donor, the newly formed FeO–H bond becomes exceedingly stronger. But what is the factor that is responsible for the bond strength variation itself? Based on thermochemical cycles,[2b,13,14a] the BDE(FeO–H) can be expressed as follows by using the common expression in solvent [Eq. (1)] and the less common in the gas phase [Eq. (2)]:

$$\mathrm{BDE(FeO{-}H)_{solv}} = 23.06E^0(\mathrm{Cpd\ I}) + 1.37\,\mathrm{p}K_a(\mathrm{Cpd\ II}) + 57 \quad (1)$$

$$\mathrm{BDE(FeO{-}H)_{gas}} = \mathrm{EA(Cpd\ I)} + \Delta G_{\mathrm{acid}}(\mathrm{Cpd\ II}) + \mathrm{IP(H)} \quad (2)$$

In Equation (1), E^0 is the one-electron reduction [eV] of Cpd I and pK_a is the acidity constant leading to the reduced Cpd I, namely Cpd II, plus a proton. The value of 57 kcal mol^{-1} is the standard hydrogen electrode potential. This equation is a measure of the basicity of Cpd II. Similarly, in Equation (2), EA is the electron affinity of Cpd I, ΔG_{acid} is dissociation energy of FeO–H to Cpd II and a proton, and IP(H) is the ionization potential of the H atom. This equation is the measure for the gas phase basicity of Cpd II.

Is it the electron affinity of Cpd I (the reduction potential) or the proton basicity of the Cpd II species, $[(Por)Fe^{IV}(O)(X)]$, that dominates the BDE(FeO–H)] value? The calculations revealed a lesser correlation with the Cpd I electron affinity (Figure S4), but the basicity of Cpd II gave a good correlation (Figure S5). It follows, therefore, that the variation of BDE(FeO–H) is primarily controlled by the variation in the basicity of Cpd II. Thus, whereas the reactivity exhibits TSR, the differentiating factor of the anionic axial ligand on reactivity is exerted through the basicity of Cpd II, as postulated by Green et al.[2b,18]

The basicity, however, does not account for the reactivity patterns in oxo-transfer reactions (e.g., epoxidation, sulfoxidation, etc). To understand the observed trends in these reactions, we computed the effect of the anionic axial ligand on BDE(Fe=O). Figure 5a shows that there is an inverse re-

lationship between BDE(Fe=O) and BDE(FeO–H), whereas Figure 5b shows that, as the ligand becomes a better electron donor, the Fe=O bond becomes weaker. For $X^- =$ $CF_3SO_3^-$ through to $X^- = HO^-$, the BDE difference was 15 kcal mol^{-1}. Therefore, as the anionic ligand in Cpd I becomes a better electron donor, it exerts two effects: i) it strengthens the FeO–H bond and thereby enhances H-abstraction activity and ii) it weakens the Fe=O bond and thereby encourages oxo-transfer reactivity. Both are straightforward BEP effects.[13,14a,17]

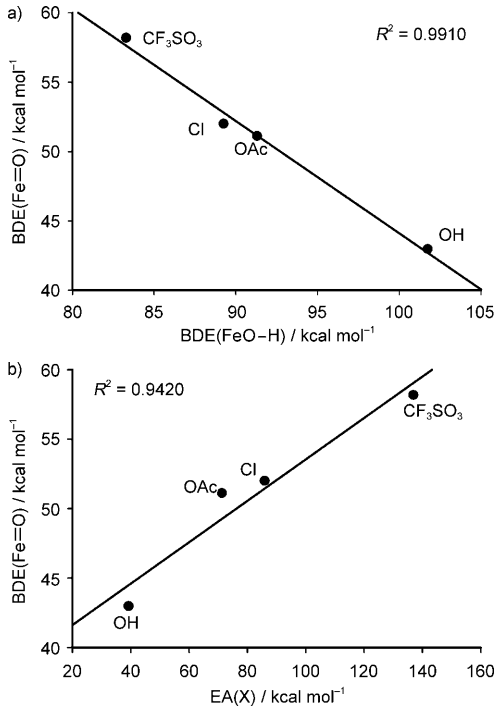

Figure 5. a) BDE of Fe=O versus BDE of FeO–H (the respective bond dissociations to the most stable spin states). b) BDE of Fe=O versus electron affinities of axial-ligand radicals.

The second set of calculations for $[(tmp)^{+\bullet}Fe^{IV}(O)(p\text{-Y-PyO})]^+$ with PhEt also gave the familiar TSR with two closely lying doublet (LS) and quartet (HS) profiles, as shown in Figure 6a.[3c] It can be seen that the barriers in the HS or LS profiles are rather close for both substituents in *p*-Y-PyO, where Y = Me and Cl. This is in agreement with the experimental results for H-abstraction from PhEt (Table S1), which show that the relative rates for *p*-Me/*p*-Cl is only about 5, corresponding to less than 0.8 kcal mol^{-1} in barrier differences. To ascertain the root cause of the close relative reactivities, we calculated the BDE(FeO–H). At the highest computational level (Table S9), the BDE values were virtually identical, 88.6 kcal mol^{-1} (*p*-Me) and 88.4 kcal mol^{-1} (*p*-Cl), in line with the experimentally observed small reactivity differences. In this case, the two components of BDE(FeO–H) [Eq. (2)] are mutually and inversely dependent leading to the calculated constancy of BDE(FeO–H). It is clear that

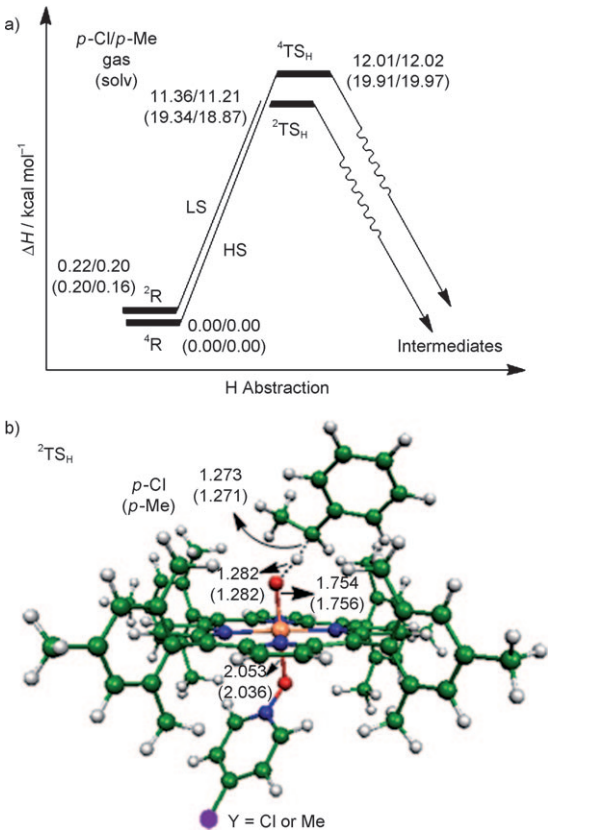

Figure 6. a) Reaction profiles and b) TSs on doublet (LS) and quartet (HS) of H-abstraction of ethylbenzene by $[(tmp)^{+\bullet}Fe^{IV}O(p\text{-Y-PyO})]^+$.

the BEP principle is not at work[17c,d] and the correlation with either component will be meaningless.

Still, however, if the FeO–H bond strength does not respond to the electron-donating/withdrawing character of the ligand, why does the experimentally observed pattern for the *p*-Y-PyO ligands follow the same direction as that observed for anionic ligands? Here we need a word of caution: the accuracy of theoretical barriers is not sufficient to distinguish cases with such close reactivity as observed in experiments. With this caveat in mind, we can try to see if theory can give us any insight into the experimental observations. Thus, it is evident from Figure 6a that the barriers for the HS process for the two substituents are either identical or in the wrong direction and, hence, in mismatch with experimental trends. As such, we certainly cannot invoke a single-state reactivity on the HS surface as being the factor behind the observed data. We note, however, that the LS ^2TS_H species exhibits a small preference for the *p*-Me substituent over *p*-Cl and therefore the observed trend may be rooted in TSR.[3c,5a,19] We may therefore consider a TSR scenario wherein the reactions start on the HS surface and cross over to the LS state, and either passes through ^2TS_H on the LS state or proceeds by a blended reactivity, passing mostly through ^2TS_H with some fraction of ^4TS_H; a fraction that is larger for the donor substituents. The data for the first scenario is apparent from Figure 6a. Here the net LS barrier

(in solution) is greater for *p*-Cl than for *p*-Me by 0.47 kcal mol^{-1} at the highest level (basis set B2) that includes ZPE, thermal, and solvation correction. If we allow for blending of the ^4TS_H path in a manner that depends on the ^2TS_H–^4TS_H gap, the effective barrier difference will be somewhat larger. Thus, while we cannot find a clear reason why the TSR barriers follow the observed experimental trend, we can say that the observed small rate enhancement by the electron donor substituents cannot be rooted in a single state HS reactivity (since the ^4TS_H species in Figure 6a exhibit, if at all, an opposite trend), but it can originate if the LS path is followed after crossover from the HS ground state of Cpd I. Since the HS–LS difference for the Cpd I reactant does not depend on the *p*-Y substituents, then this small reactivity difference must arises from the energy difference of the ^2TS_H species for the two cases. These species shown in Figure 6b exhibit tiny geometric differences, for example, in the extent of C–H bond cleavage and in the Fe–OPy bond lengths, which are slightly longer for the *p*-Cl species. There might be other less visible deformations and one way to assess the feasibility of this factor is to calculate the total deformation energies (ΔE_{def}(tot)) in the two ^2TS_H species, where ΔE_{def}(tot) is the sum of the deformation of the Cpd I and PhEt moieties relative to their ground states. In doing so, we find that the ^2TS_H(*p*-Me) has a lower deformation energy than the ^2TS_H(*p*-Cl) by 0.2 kcal mol^{-1} in the gas phase, which is approximately equal to the computed gas-phase barrier difference of the two reactions on the LS surface. We may therefore cautiously conclude that the small preference for the TSR reactivity of $[(tmp)^{+\bullet}Fe^{IV}(O)(p\text{-Me-PyO})]^+$ over $[(tmp)^{+\bullet}Fe^{IV}(O)(p\text{-Cl-PyO})]^+$ in H-abstraction from PhEt originates in the lower deformation energy required to reach the transition state, augmented by solvation contribution.

While we have not calculated other reactions, we may still note that oxo-transfer reactions, such as sulfoxidation, proceed through LS TSs[21] and in general C=C epoxidation and aromatic hydroxylation[10,22] all have lower lying LS TSs, as in the case shown in Figure 6a. Therefore, within the aforementioned caveat of computational accuracy, the TSR scenario might provide a rationale for the observed reactivity patterns in the present study.

Conclusion

This paper presents experimental and theoretical results on the axial ligand effects of iron(IV)-oxo porphyrin π-cation radical species in oxo-transfer and H-atom abstraction reactions, such as olefin epoxidation, aromatic hydroxylation, alcohol oxidation, and alkane hydroxylation. We found that iron(IV)-oxo porphyrin π-cation radicals bearing electron-donating axial ligands are more reactive in the oxo-transfer and hydrogen-atom abstraction reactions. This finding was reproduced by DFT calculations for a series of anionic axial ligands and two neutral *p*-Y-PyO ligands. The combination of experiment and theory enabled us to elucidate the following two axial ligand effects in oxygenation reactions by heme-based Cpd I species.

a) In a series of anionic axial ligands, as the ligand becomes a better electron donor, it leads to the following two effects: i) it strengthens the FeO–H bond and thereby enhances H-abstraction activity and ii) it weakens the Fe=O bond and encourages oxo-transfer reactivity. Both are straightforward BEP effects.[13,14a,17]
b) In contrast, in a series of neutral ligands with probe substituents, such as *p*-Y-PyO, there is a relatively weak trend that appears to be an outcome of TSR.[3c,19]

While Nature's selection of thiolate in P450 enzyme belongs to the effect in a), this is not generally the dominant factor since, in addition, to the two effects (a and b) there is an electrophilicity-dominated trend that is expressed through TS stabilization, as outline recently in the H-abstraction from *N,N*-dimethylanilines.[17c] The last effect opposes the other two and hence generates the rich reactivity patterns observed so far. The recent modelling of C–H activation by Cpd I incorporates all the effects in a single model of barrier formation.[17c]

Experimental and Computational Methods

Materials: Commercially available reagents were of the best available purity and were used without further purification unless otherwise noted. Acetonitrile (CH_3CN) and dichloromethane (CH_2Cl_2) were dried according to the literature procedures and distilled under Ar prior to use.[23] Pyridine *N*-oxide and its derivatives were obtained from Aldrich Chemical Co. and used without further purification. *m*-Chloroperbenzoic acid (*m*-CPBA) was purified by washing with phosphate buffer (pH 7.4) followed by water and then dried under reduced pressure.[24] $[Fe^{III}(tmp)]Cl$ was purchased from Frontier Scientific Inc. (Logan, UT, USA). $[Fe^{III}(tmp)](CF_3SO_3)$ was prepared by stirring equimolar amounts of $[Fe^{III}(tmp)]Cl$ and $AgCF_3SO_3$, followed by filtration through a 0.45 μM filter; the resulting solution was used immediately. The deuterated substrate, xanthene-d_2, was prepared by taking xanthene (0.5 g, 2.7 mmol) in $[D_6]$DMSO (3 mL) along with NaH (0.2 g, 8.1 mmol) under an inert atmosphere.[25] After the deep red solution was stirred at room temperature for 8 h, the reaction was quenched with D_2O (5 mL). The crude product was filtered and washed with copious amounts of H_2O. ^1H NMR confirmed > 99 % deuteration.

Instrumentation: UV/Vis spectra were recorded on a Hewlett Packard 8453 spectrophotometer equipped with a circulating water bath or with an Optostat variable-temperature liquid-nitrogen cryostat (Oxford instruments) at 0 °C. Ozone was generated by electric discharge of oxygen gas with an O1 (Pacific Ozone) and used without further purification. Product analysis was performed with an Agilent Technologies 6890N gas chromatograph equipped with a FID detector (GC) and Thermo Finnigan (Austin, Texas, USA) FOCUS DSQ (dual stage quadrupole) mass spectrometer interfaced with Finnigan FOCUS gas chromatograph (GC-MS). EPR spectra were obtained on a JEOL JES-FA200 spectrometer. ^1H NMR spectra were measured with Bruker DPX-250 spectrometer.

Kinetics studies: Reactions were followed by monitoring UV/Vis spectral changes of reaction solutions at −40 °C. All reactions were run, at least, in triplicate and the data reported represents the average of these reactions. Iron(IV)-oxo porphyrin π-cation radicals bearing *p*-substituted pyridine *N*-oxides (*p*-Y-PyO), $[(tmp)^{+\bullet}Fe^{IV}(O)(p\text{-Y-PyO})]^+$ (**1**-Y) (Y =

OCH_3, CH_3, H, Cl) were prepared by literature methods: $[Fe^{III}(tmp)](CF_3SO_3)$ was treated with 5 equivalents of *p*-Y-PyO, followed by the bubbling of ozone gas slowly into a solvent mixture of CH_3CN and CH_2Cl_2 (9:1) at −40 °C[4b,26] or by reacting with 1.1 equivalents of *m*-CPBA in a solvent mixture of CH_3CN and CH_2Cl_2 (9:1) at −40 °C.[4c] The formation of the iron-oxo intermediates was confirmed by UV/Vis and EPR spectroscopies. Subsequently, appropriate amounts of substrates were added to the reaction solutions. After the completion of reactions, pseudo-first-order fitting of the kinetic data allowed us to determine k_{obs} values. Product analysis was performed with $[(tmp)^{+\bullet}Fe^{IV}(O)(p\text{-Y-PyO})]^+$ (**1**-Y) (2 mM) and cyclohexene (0.2 M) at −40 and −80 °C by injecting the reaction solutions directly into GC and GC-MS. Products were identified by comparing retention times and mass patterns to those of known authentic samples. Cyclohexene oxide (52%) was formed as a major product with small amounts of cyclohexenol (<4%) and cyclohexenone (<5%). Product yields were determined by comparison against standard curves prepared with authentic samples and by using decane as an internal standard.

The spin states of $[(tmp)^{+\bullet}Fe^{IV}(O)]^+$, $[(tmp)^{+\bullet}Fe^{IV}(O)(p\text{-H-PyO})]^+$, and $[(tmp)^{+\bullet}Fe^{IV}(O)(p\text{-Cl-PyO})]^+$ intermediates were determined using the modified ^{1}H NMR Evans method at −40 °C.[27] The magnetic moments (μ_B) calculated were 4.6, 4.7, and 4.6 B.M. for $[(tmp)^{+\bullet}Fe^{IV}(O)]^+$, $[(tmp)^{+\bullet}Fe^{IV}(O)(p\text{-H-PyO})]^+$, and $[(tmp)^{+\bullet}Fe^{IV}(O)(p\text{-Cl-PyO})]^+$, respectively. These μ_B values indicate that the spin-states of all intermediates measured are high-spin $S=3/2$ states at −40 °C.

Computational methods: All computations were carried out using the B3LYP functional.[28] The geometries were optimized with the double-ζ LACVP basis set (B1),[29] followed by single-point energy correction with larger basis set B2. In the activation energy calculations for $[(Por)^{+\bullet}Fe^{IV}(O)(X)]$ systems, our B2 basis set was: LACV3P+* for iron, 6-311+G* for electronegative atoms,[30] and 6-31G* for C and H atoms. In all BDE calculations, B2 was the same as described above except the H atom in Fe−OH moiety, for which 6-311++G** was used. For activation energy calculations of the $[(tmp)^{+\bullet}Fe^{IV}(O)(p\text{-Y-PyO})]^+$ reactions, B2 is same as above except for the use of 6-311G** for all C and H atoms. Transition states and optimized minima were characterized by frequency calculations as having one and zero imaginary vibrational models, respectively. The solvent effect was computed with the polarizable continuum model (PCM) calculation in Gaussian03 program[31] with two cavity building models; the United Atom models of UAHF and UAKS. Acetonitrile was used as the solvent in the PCM calculation. An additional sphere on the transferred H atom was added in the cavity building of PCM calculation. Our energies include ZPE and thermal corrections (at −40 °C), but not entropic corrections due to loss of rotational and translation degrees of freedom, which are overestimated by current programs and assume a complete loss of these degrees of freedom.

Due to the spin contamination of the doublet state, we applied the Yamaguchi's spin projected correction[32] for our calculated energy of the symmetry-broken doublet state as shown below:

$$E_s = (E_C - aE_{S+1})/(1-a),\ a = [< S^2 >_C - s(s+1)]/2(s+1) \quad (3)$$

E_C is the spin-contaminated energy for doublet state, E_{S+1} is the energy for quartet state (it has only small spin contamination), $<S^2>_C$ is the calculated spin expectation value of the spin-contaminated doublet state. The reliability of EA(X) calculations was verified against experimental values.[33–36]

Acknowledgements

The research at EWU was supported by the Korea Science and Engineering Foundation through the Creative Research Initiatives Program (to W.N.) and KOSEF/MEST through WCU project (R31-2008-000-10010-0) (to S.S. and W.N.). The research at the HU was supported by the Ministry of Education and Research within the Framework of the German-Israeli Project Cooperation (DIP). H.C. thanks the Golda Meir fellowship fund.

[1] a) P. R. Ortiz de Montellano, *Cytochrome P450: Structure, Mechanism, and Biochemistry*, 3rd ed., Kluwer Academic, New York, **2005**; b) I. G. Denisov, T. M. Makris, S. G. Sligar, I. Schlichting, *Chem. Rev.* **2005**, *105*, 2253–2277; c) B. Meunier, S. P. de Visser, S. Shaik, *Chem. Rev.* **2004**, *104*, 3947–3980; d) S. Shaik, D. Kumar, S. P. de Visser, A. Altun, W. Thiel, *Chem. Rev.* **2005**, *105*, 2279–2328.

[2] a) R. K. Behan, M. T. Green, *J. Inorg. Biochem.* **2006**, *100*, 448–459; b) M. T. Green, J. H. Dawson, H. B. Gray, *Science* **2004**, *304*, 1653–1656; c) J. H. Dawson, *Science* **1988**, *240*, 433–439; d) F. Ogliaro, S. P. de Visser, S. Shaik, *J. Inorg. Biochem.* **2002**, *91*, 554–567.

[3] a) R. van Eldik, *Coord. Chem. Rev.* **2007**, *251*, 1649–1662; b) W. Nam, *Acc. Chem. Res.* **2007**, *40*, 522–531; c) S. Shaik, H. Hirao, D. Kumar, *Acc. Chem. Res.* **2007**, *40*, 532–542.

[4] a) Z. Gross, S. Nimri, *Inorg. Chem.* **1994**, *33*, 1731–1732; b) W. J. Song, Y. O. Ryu, R. Song, W. Nam, *J. Biol. Inorg. Chem.* **2005**, *10*, 294–304; c) A. Takahashi, T. Kurahashi, H. Fujii, *Inorg. Chem.* **2009**, *48*, 2614–2625; d) T. Kamachi, T. Kouno, W. Nam, K. Yoshizawa, *J. Inorg. Biochem.* **2006**, *100*, 751–754; e) S. P. de Visser, *J. Biol. Inorg. Chem.* **2006**, *11*, 168–178; f) R. Wang, S. P. de Visser, *J. Inorg. Biochem.* **2007**, *101*, 1464–1472.

[5] a) N. Hessenauer-Ilicheva, A. Franke, D. Meyer, W.-D. Woggon, R. van Eldik, *Chem. Eur. J.* **2009**, *15*, 2941–2959; b) N. Hessenauer-Ilicheva, A. Franke, D. Meyer, W.-D. Woggon, R. van Eldik, *J. Am. Chem. Soc.* **2007**, *129*, 12473–12479; c) A. Franke, G. Stochel, N. Suzuki, T. Higuchi, K. Okuzono, R. van Eldik, *J. Am. Chem. Soc.* **2005**, *127*, 5360–5375; d) N. Suzuki, T. Higuchi, T. Nagano, *J. Am. Chem. Soc.* **2002**, *124*, 9622–9628; e) T. Ohno, N. Suzuki, T. Dokoh, Y. Urano, K. Kikuchi, M. Hirobe, T. Higuchi, T. Nagano, *J. Inorg. Biochem.* **2000**, *82*, 123–125; f) T. Higuchi, K. Shimada, M. Maruyama, M. Hirobe, *J. Am. Chem. Soc.* **1993**, *115*, 7551–7552.

[6] C. V. Sastri, J. Lee, K. Oh, Y. J. Lee, J. Lee, T. A. Jackson, K. Ray, H. Hirao, W. Shin, J. A. Halfen, J. Kim, L. Que, Jr., S. Shaik, W. Nam, *Proc. Natl. Acad. Sci. USA* **2007**, *104*, 19181–19186.

[7] H. Hirao, L. Que, Jr., W. Nam, S. Shaik, *Chem. Eur. J.* **2008**, *14*, 1740–1756.

[8] S. N. Dhuri, M. S. Seo, Y.-M. Lee, H. Hirao, Y. Wang, W. Nam, S. Shaik, *Angew. Chem.* **2008**, *120*, 3404–3407; *Angew. Chem. Int. Ed.* **2008**, *47*, 3356–3359.

[9] a) J. T. Groves, Z. Gross in *Bioinorganic Chemistry: An Inorganic Perspective of Life* (Ed.: D. P. Kessissoglou), Kluwer Academic, Dordrecht, **1995**, pp. 39–47; b) M. H. Lim, S. W. Jin, Y. J. Lee, G.-J. Jhon, W. Nam, C. Kim, *Bull. Korean Chem. Soc.* **2001**, *22*, 93–96; c) A. Takahashi, T. Kurahashi, H. Fujii, *Inorg. Chem.* **2007**, *46*, 6227–6229.

[10] a) M.-J. Kang, W. J. Song, A.-R. Han, Y. S. Choi, H. G. Jang, W. Nam, *J. Org. Chem.* **2007**, *72*, 6301–6304; b) S. P. de Visser, *Chem. Eur. J.* **2006**, *12*, 8168–8177; c) S. P. de Visser, S. Shaik, *J. Am. Chem. Soc.* **2003**, *125*, 7413–7424.

[11] N. Y. Oh, Y. Suh, M. J. Park, M. S. Seo, J. Kim, W. Nam, *Angew. Chem.* **2005**, *117*, 4307–4311; *Angew. Chem. Int. Ed.* **2005**, *44*, 4235–4239.

[12] Y. J. Jeong, Y. Kang, A.-R. Han, Y.-M. Lee, H. Kotani, S. Fukuzumi, W. Nam, *Angew. Chem.* **2008**, *120*, 7431–7434; *Angew. Chem. Int. Ed.* **2008**, *47*, 7321–7324.

[13] a) J. P. Roth, J. M. Mayer, *Inorg. Chem.* **1999**, *38*, 2760–2761; b) J. M. Mayer, *Biomimetic Oxidations Catalyzed by Transition Metal Complexes* (Ed.: B. Meunier), Imperial College Press, London, **2000**, pp. 1–43.

[14] a) J. M. Mayer, *Acc. Chem. Res.* **1998**, *31*, 441–450; b) A. S. Borovik, *Acc. Chem. Res.* **2005**, *38*, 54–61; c) W. W. Y. Lam, S.-M. Yiu, D. T. Y. Yiu, T.-C. Lau, W.-P. Yip, C.-M. Che, *Inorg. Chem.* **2003**, *42*, 8011–8018; d) C. R. Goldsmith, A. P. Cole, T. D. P. Stack, *J. Am. Chem. Soc.* **2005**, *127*, 9904–9912; e) S. P. de Visser, D. Kumar, S. Shaik, *J. Am. Chem. Soc.* **2004**, *126*, 8362–8363.

[15] a) C. Li, W. Wu, D. Kumar, S. Shaik, *J. Am. Chem. Soc.* **2006**, *128*, 394–395; b) Y. Moreau, H. Chen, E. Derat, H. Hirao, C. Bolm, S. Shaik, *J. Phys. Chem. B* **2007**, *111*, 10288–10299.

[16] We were not able to determine the KIE value in ethylbenzene hydroxylation since the reaction rate of **1**-Y with deuterated [D_{10}]ethylbenzene was similar to that of the natural decay of **1**-Y: Z. Pan, J. H. Horner, M. Newcomb, *J. Am. Chem. Soc.* **2008**, *130*, 7776–7777.

[17] a) R. P. Bell, *Proc. R. Soc. London Ser. A* **1936**, *154*, 414–421; b) M. G. Evans, M. Polanyi, *Trans. Faraday. Soc.* **1938**, *34*, 11–24; c) For comments on the limitations of the principle, see recent VB modelling of C-H hydroxylation in: S. Shaik, D. Kumar, S. P. de Visser, *J. Am. Chem. Soc.* **2008**, *130*, 10128–10140; d) For general comments on rate-equilibrium relations, see A. Pross, S. S. Shaik, *New J. Chem.* **1989**, *13*, 427–433.

[18] a) M. T. Green, *J. Am. Chem. Soc.* **2006**, *128*, 1902–1906; b) R. K. Behan, L. M. Hoffart, K. L. Stone, C. Krebs, M. T. Green, *J. Am. Chem. Soc.* **2006**, *128*, 11471–11474.

[19] D. Schröder, S. Shaik, H. Schwarz, *Acc. Chem. Res.* **2000**, *33*, 139–145.

[20] The spin states of $[(tmp)^{+\cdot}Fe^{IV}(O)]^+$, $[(tmp)^{+\cdot}Fe^{IV}(O)(p\text{-H-PyO})]^+$ and $[(tmp)^{+\cdot}Fe^{IV}(O)(p\text{-Cl-PyO})]^+$ were determined to be $S=3/2$ in CH_3CN at $-40\,^{\circ}C$ (see the Supporting Information, Experimental Section): a) D. Mandon, R. Weiss, K. Jayaraj, A. Gold, J. Terner, E. Bill, A. X. Trautwein, *Inorg. Chem.* **1992**, *31*, 4404–4409; b) B. Boso, G. Lang, T. J. McMurry, J. T. Groves, *J. Chem. Phys.* **1983**, *79*, 1122–1126.

[21] a) P. Rydberg, U. Ryde, L. Olsen, *J. Chem. Theory Comput.* **2008**, *4*, 1369–1377; b) C. Li, L. Zhang, C. Zhang, H. Hirao, W. Wu, S. Shaik, *Angew. Chem.* **2007**, *119*, 8316–8318; *Angew. Chem. Int. Ed.* **2007**, *46*, 8168–8170.

[22] C. M. Bathelt, L. Ridder, A. J. Mulholland, J. N. Harvey, *J. Am. Chem. Soc.* **2003**, *125*, 15004–15005.

[23] W. L. F. Armarego, C. L. L. Chai, *Purification of Laboratory Chemicals*, 5th ed., Butterworth-Heiemann, Oxford, **2003**.

[24] O. Bortolini, S. Campestrini, F. Di Furia, G. Modena, *J. Org. Chem.* **1987**, *52*, 5093–5095.

[25] C. R. Goldsmith, R. T. Jonas, T. D. P. Stack, *J. Am. Chem. Soc.* **2002**, *124*, 83–96.

[26] Z. Gross, S. Nimri, L. Simkhovich, *J. Mol. Catal. A* **1996**, *113*, 231–238.

[27] D. F. Evans, D. A. Jakubovic, *J. Chem. Soc. Dalton Trans.* **1988**, 2927–2933.

[28] a) A. D. Becke, *Phys. Rev. A* **1988**, *38*, 3098–3100; b) C. Lee, W. Yang, R. G. Parr, *Phys. Rev. B* **1988**, *37*, 785–789; c) A. D. Becke, *J. Chem. Phys.* **1993**, *98*, 5648–5652; d) A. D. Becke, *J. Chem. Phys.* **1993**, *98*, 1372–1377.

[29] LACVP is constructed from the LANL2DZ basis sets: a) J. P. Hay, W. R. Wadt, *J. Chem. Phys.* **1985**, *82*, 299–310; b) R. A. Friesner, R. B. Murphy, M. D. Beachy, M. N. Ringlanda, W. T. Pollard, B. D. Dunietz, Y. X. Cao, *J. Phys. Chem. A* **1999**, *103*, 1913–1928.

[30] W. J. Hehre, R. Ditchfield, J. A. Pople, *J. Chem. Phys.* **1972**, *56*, 2257–2261.

[31] Gaussian 03, Revision C.02, M. J. Frisch, G. W. Trucks, H. B. Schlegel, G. E. Scuseria, M. A. Robb, J. R. Cheeseman, J. A. Montgomery, Jr., T. Vreven, K. N. Kudin, J. C. Burant, J. M. Millam, S. S. Iyengar, J. Tomasi, V. Barone, B. Mennucci, M. Cossi, G. Scalmani, N. Rega, G. A. Petersson, H. Nakatsuji, M. Hada, M. Ehara, K. Toyota, R. Fukuda, J. Hasegawa, M. Ishida, T. Nakajima, Y. Honda, O. Kitao, H. Nakai, M. Klene, X. Li, J. E. Knox, H. P. Hratchian, J. B. Cross, V. Bakken, C. Adamo, J. Jaramillo, R. Gomperts, R. E. Stratmann, O. Yazyev, A. J. Austin, R. Cammi, C. Pomelli, J. W. Ochterski, P. Y. Ayala, K. Morokuma, G. A. Voth, P. Salvador, J. J. Dannenberg, V. G. Zakrzewski, S. Dapprich, A. D. Daniels, M. C. Strain, O. Farkas, D. K. Malick, A. D. Rabuck, K. Raghavachari, J. B. Foresman, J. V. Ortiz, Q. Cui, A. G. Baboul, S. Clifford, J. Cioslowski, B. B. Stefanov, G. Liu, A. Liashenko, P. Piskorz, I. Komaromi, R. L. Martin, D. J. Fox, T. Keith, M. A. Al-Laham, C. Y. Peng, A. Nanayakkara, M. Challacombe, P. M. W. Gill, B. Johnson, W. Chen, M. W. Wong, C. Gonzalez, J. A. Pople, Gaussian, Inc., Wallingford CT, **2004**.

[32] K. Yamaguchi, F. Jensen, A. Dorigo, K. N. Houk, *Chem. Phys. Lett.* **1988**, *149*, 537–542.

[33] R. J. Celotta, R. A. Bennett, J. L. Hall, *J. Chem. Phys.* **1974**, *60*, 1740–1745.

[34] X. B. Wang, H. K. Woo, L. S. Wang, B. Minofar, P. Jungwirth, *J. Phys. Chem. A* **2006**, *110*, 5047–5050.

[35] H. Hotop, W. C. Lineberger, *J. Phys. Chem. Ref. Data* **1975**, *4*, 539–576.

[36] M. J. Blandamer, M. F. Fox, *Chem. Rev.* **1970**, *70*, 59–93.

Received: May 10, 2009
Published online: August 20, 2009

